Supporting Materials for

Force-Induced Unfolding of Leucine-Rich Repeats of Glycoprotein Ibα Strengthens Ligand Interaction

Lining Ju,[1,3,4,5,*] Jizhong Lou,[6] Yunfeng Chen,[2,3] Zhenhai Li,[7] and Cheng Zhu[1,2,3,*]

[1]Coulter Department of Biomedical Engineering, [2]Woodruff School of Mechanical Engineering, and [3]Petit Institute for Bioengineering and Biosciences, Georgia Institute of Technology, Atlanta, Georgia; [4]Heart Research Institute and [5]Charles Perkins Centre, The University of Sydney, Camperdown, New South Wales, Australia; [6]Laboratory of RNA Biology, Institute of Biophysics, Chinese Academy of Sciences, Beijing, China; and [7]Quantum Beam Science Directorate, Japan Atomic Energy Agency, Kizugawa, Kyoto, Japan

Supplementary Figure S1

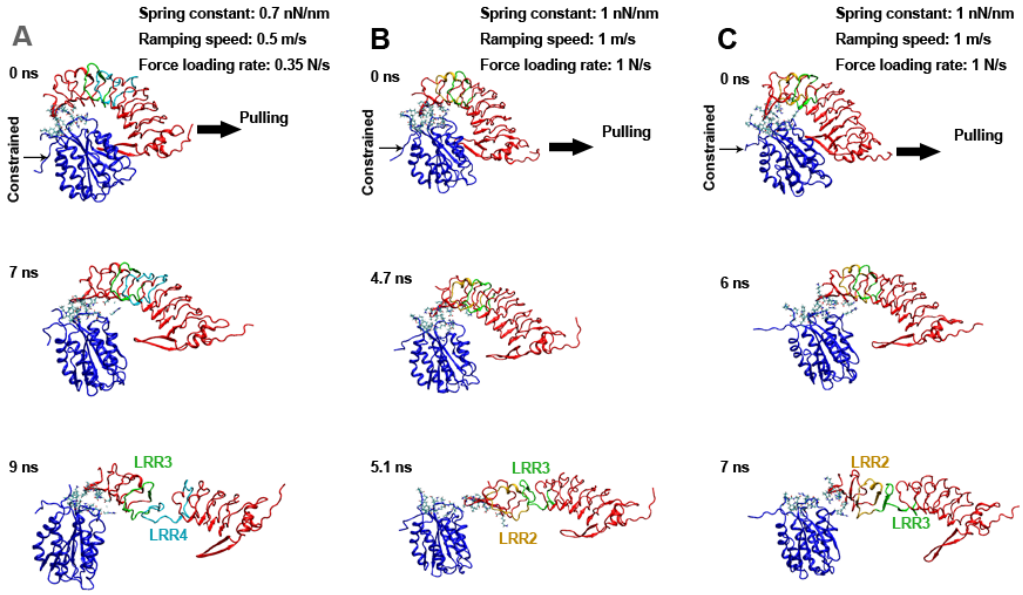

Supplementary Figure S1, corresponding to Fig. 1. Sequential snapshots of three SMD simulations of GPIbαN dissociation from the A1 domain under different conditions. Upper, middle, and lower panels in each row represent, respectively, the moment when simulation began, GPIbαN (red) β-switch dissociated from the A1 (blue) central β-sheet, and LRRs unfolded. The constrained atom in A1 was either the residue C1272, Cα (A and C), or the residue H1268, C12 (B). The ramping speed was 0.7 m/s (A) or 1 m/s (B and C). The force loading point and pulling direction are indicated.

Materials and methods

SMD simulations.

SMD simulations were performed using the NAMD program with the CHARMM22 all-atom force field for protein as previously described (1). Briefly, The X-ray crystal structure of the A1–GPIbαN complex (Protein Data Bank code 1SQ0 (2)) was used as the initial structure, which was put in a 160 Å × 96 Å × 72 Å water box with 10 Na^+ and 21 Cl^- ions to neutralize the system, which contained 140,570 atoms. The system was subjected to 10,000 steps of energy minimization with heavy atoms fixed and another 10,000 steps with all atoms free. The system was heated gradually from 0-300K in 0.1 ns and then equilibrated for 3 ns with pressure and temperature control. The temperature was held at 300K using Langevin dynamics, and the pressure was held at 1 atm by the Langevin piston method. The equilibrated structure was taken as the starting point for SMD simulations. In SMD, the Cα atom of the A1 N-terminal residue H1268, C12 (Fig. 1 and Fig. S1B) or C1272, Cα (in Fig. S1A and C) was harmonically constrained and the Cα atom of the GPIbα C-terminal residue L267 was pulled at a constant ramping speed of 0.5 m/s (Fig. 1 and Fig. S1A) or 1 m/s (Fig. S1B and C) with spring constant of 0.7 nN/nm (Fig. 1 and Fig. S1A) or 1 nN/nm (Fig. S1B and C). We adjusted ramping speeds and spring constants in order to accelerate the processes, so that unbinding could be observed in 10–15 ns of the simulation time. Although the pulling speed used in MD simulations was several order of magnitude higher than those used in experiments and in blood flow, the results from MD simulations have been confirmed by force spectroscopy, suggesting the validity of MD simulations (3). Structures in Fig. 1 and S1 were generated using VMD (4).

Purification of platelets and red blood cells

Platelets and red blood cells (RBCs) were isolated from 3 ml venous blood drawn from healthy adult donors abiding the protocol approved by the Georgia Institute of Technology Institutional Review Board. Whole blood was first collected in a 1:10 ACD buffer (6.25 g sodium citrate, 3.1 g citric acid anhidrous, 3.4 g D-glucose in 250

ml H_2O, pH 6.7) and centrifuged at 150 g for 15 min at room temperature. Platelet-rich plasma (from the top yellow layer) was then centrifuged at 900 g for 5 min. The platelet pellet was gently resuspended in the HEPES-Tyrode buffer (134 mM NaCl, 12 mM NaHCO3, 2.9 mM KCl, 0.34 mM NaH_2PO_4, 5 mM HEPES, and 5 mM D-glucose, 1% Bovine serum albumin, pH 7.4) as the washed platelets (5). To avoid unwanted platelet activation by RBC released ADP, apyrase (0.01 U/mL) was added to the final platelet suspension.

RBCs (3 μl, from the bottom red layer) were resuspended in a carbonate/bicarbonate buffer (0.1M $NaHCO_3$ and Na_2CO_3, pH 8.5) and then biotinylated by covalently linking polymer biotin-PEG3500-SGA (JenKem USA, TX) with a 30 min incubation at room temperature (6). To balloon RBCs for the force probe use in the Tyrode buffer of physiological osmolarity, RBCs were further incubated with nystatin (Sigma-Aldrich) in an N2-5% buffer (265.2 mM KCl, 38.8 mM NaCl, 0.94 mM KH_2PO_4, 4.74 mM Na_2HPO_4, 27 mM sucrose; pH 7.2, 588 mOsm) for 30 min at 0°C. The modified RBCs were washed twice with the N2 buffer and resuspended in the N2 buffer for the BFP experiments (7).

Proteins and antibodies

Recombinant wild-type (WT) monomeric VWF-A1 (residues 1238-1471) generated by E.coli as previously described (5, 8) was a generous gift of Miguel A. Cruz (Baylor College of Medicine). Glycocalicin (GC, extracellular portion of GPIbα) was cleaved and purified from outdated platelets (Blood bank at Emory university) as described previously (9, 10). GC covers most of the GPIbα extracellular portion, consisting of the A1-binding domain GPIbαN and a long megaglycopipetide stalk (Fig. 2G). The GPIbαN zoom-in includes a N-terminal β-finger (residues 1-18, orange), eight LRRs (19–208, brown for repeats with A1 contacts and green for those without), a disulfide knot structure (209–265) including the C-terminal β-switch (227-240, blue), and a C-terminal anionic region (266–280, magenta) (Fig. 1). Two anti-GPIbα mAbs were purchased: HIP1(Abcam) and SZ2 (Santa Cruz Biotechnology). Anti-A1 mAb 5D2 was a gift from Dr. Michael Berndt (Curtin University, WA, Australia).

Functionalization of glass beads

Proteins (A1, GC and mAbs) were covalently modified with maleimide-PEG3500-NHS (MW ~3500 Da; JenKem, TX) in the carbonate/bicarbonate buffer. To coat maleimized proteins on glass beads, 2-μm (diameter) silanized borosilicatebeads (Thermo Scientific) were first covalently coupled with mercapto-propyl-trimethoxy silane (Sigma), followed by covalently linking to both streptavidin-maleimide (Sigma) and maleimide modified proteins in monobasic/dibasic phosphate buffer (0.2M NaH_2PO_4 and Na_2HPO_4, pH 6.8) (Fig. 2B, left). After overnight incubation and resuspending in phosphate buffer with 1% human serum albumin, beads were ready for immediate use in BFP experiments. The specificity and functional effect were justified in the previous study (5).

BFP experiments

Our BFP experimental procedure used to study VWF–GPIbα interaction has been described (5) with a default spring constant at 0.25 pN/nm. In each test cycle, the target (GC coated bead, Fig. 2A and B, right) was driven to approach and contact the probe (A1 or mAb coated bead, Fig. 2A and B, left) with an 18-pN compressive force for a certain contact time (1 s by default) to allow for bond formation and then was retracted at a preset ramping speed (4 μm/s by default) for adhesion detection. During the retraction, an adhesion event was signified by tensile force (>0 pN, Fig. 2C and D), but no tensile force (~0 pN) was detected in a no-adhesion event (13). The site density of either receptor or ligand was titrated low enough (<30/μm^2) on the contact area to achieve single-molecule level measurements with <20% adhesion frequency (11,13). To measure bond lifetime, the target was held at a desired clamp force (Fig. 2C, dotted line) to wait for bond dissociation and returned to the original position to complete the cycle. Lifetime was measured from the instant when the force reached the desired level to the instant of bond dissociation (Fig. 2C, red trace). To investigate the force loading rate effect (spring constant × ramping speed) on unfolding as

suggested by SMD simulations, we increased the spring constant to 3.75 pN/nm and the ramping speed to 8 μm/s (Fig. 2F) to match the respective 1.4 and 2 folds increases used in SMD (Fig. S1A vs. S1B,C). Therefore, we compared the different LRR unfolding behaviors between 1000 and 3000 pN/s force rates in experiments (Fig. 2F).

The molecular unfolding analysis was derived from a force versus extension curve (e.g., Fig. 2C inset), which was converted from force versus time data (e.g., Fig. 2C). Here, molecular extension was calculated as differential displacement between the BFP tracking system (probe positioning) and the piezoelectric actuator feedback system (target positioning) as previously described (12). The unfolding activity was signified by a sudden extension increase of >5 nm, whereas force remained or dropped. The extension length was considered as the unfolding contour length.

References:

1. Yago, T., J. Lou, T. Wu, J. Yang, J.J. Miner, et al. 2008. Platelet glycoprotein Ibalpha forms catch bonds with human WT vWF but not with type 2B von Willebrand disease vWF. J Clin Invest. 118: 3195–3207.

2. Dumas, J.J., R. Kumar, T. McDonagh, F. Sullivan, M.L. Stahl, et al. 2004. Crystal structure of the wild-type von Willebrand factor A1-glycoprotein Ibalpha complex reveals conformation differences with a complex bearing von Willebrand disease mutations. J Biol Chem. 279: 23327–23334.

3. Rico, F., L. Gonzalez, I. Casuso, M. Puig-Vidal, and S. Scheuring. 2013. High-speed force spectroscopy unfolds titin at the velocity of molecular dynamics simulations. Science. 342: 741–743.

4. Humphrey, W., A. Dalke, and K. Schulten. 1996. VMD: visual molecular dynamics. J Mol Graph. 14: 33–38.

5. Ju, L., J.-F. Dong, M.A. Cruz, and C. Zhu. 2013. The N-terminal flanking region of the A1 domain regulates the force-dependent binding of von Willebrand factor to platelet glycoprotein Ibα. J Biol Chem. 288: 32289–32301.

6. Evans, E., K. Ritchie, and R. Merkel. 1995. Sensitive force technique to probe molecular adhesion and structural linkages at biological interfaces. Biophys J. 68: 2580–2587.

7. Liu, B., W. Chen, B.D. Evavold, and C. Zhu. 2014. Accumulation of dynamic catch bonds between TCR and agonist peptide-MHC triggers T cell signaling. Cell. 157: 357–368.

8. Cruz, M.A., and R.I. Handin. 1993. The interaction of the von Willebrand factor-A1 domain with platelet glycoprotein Ib/IX. J Biol Chem. 268: 21238–21245.

9. Fox, J.E. 1985. Linkage of a membrane skeleton to integral membrane glycoproteins in human platelets. Identification of one of the glycoproteins as glycoprotein Ib. J Clin Invest. 76: 1673–1683.

10. Fox, J.E., L.P. Aggerbeck, and M.C. Berndt. 1988. Structure of the glycoprotein Ib.IX complex from platelet membranes. J Biol Chem. 263: 4882–4890.

11. Chen, W., V.I. Zarnitsyna, K.K. Sarangapani, J. Huang, and C. Zhu. 2008. Measuring Receptor–Ligand Binding Kinetics on Cell Surfaces: From Adhesion Frequency to Thermal Fluctuation Methods. Cel. Mol. Bioeng. 1: 276–288.

12. Chen, W., J. Lou, E.A. Evans, and C. Zhu. 2012. Observing force-regulated conformational changes and ligand dissociation from a single integrin on cells. J Cell Biol. 199: 497–512.

13. Ju, L., Y. Chen, F. Zhou, H. Lu, M.A. Cruz, et al. 2015. Von Willebrand factor-A1 domain binds platelet glycoprotein Ibα in multiple states with distinctive force-dependent dissociation kinetics. Thrombosis Research. 136: 606–612.